

This has an integrating factor, $\cos\gamma$, and the equation becomes

$$\frac{d}{ds}(\lambda_2 \cos\lambda) = \left[-(\lambda_1 \phi) \frac{(Vc - gH)}{VcH} \cos\gamma + \frac{C_3}{H} \cos\gamma + \frac{C_4}{H} \sin\gamma \right] \cos\gamma$$

This is integrable if, and only if

$$(\lambda_1 \phi) = \frac{Vc}{(Vc - gH)} [C_3 + C_4 \tan\gamma] \quad (27)$$

whereupon

$$\lambda_2 \cos\gamma = C_2 \quad (\text{constant}) \quad (28)$$

With respect to the algebraic variable velocity, V

$$\lambda_1 \frac{D'}{c} \left(I + \frac{V}{c} \right) \exp\left(\frac{V}{c} - \frac{y}{H}\right) - \lambda_1 \phi \frac{g}{V^2 c} \sin\gamma - \frac{2g}{V^3} (\lambda_2 \cos\gamma) - \frac{g}{V^2 c} = 0 \quad (29)$$

Hence

$$D' \frac{V}{c} \exp\left(\frac{V}{c} - \frac{y}{H}\right) = \phi \frac{g}{V(c+V)} \sin\gamma + \phi \left[\frac{2gc(\lambda_2 \cos\gamma)}{V^2(c+V)} + \frac{g}{V(c+V)} \right] \frac{I}{(\lambda_1 \phi)} \quad (30)$$

The condition for the integral to depend only on altitude and time to altitude, and not on angle turned through, is

$$\left[\frac{2gc \cdot C_2}{V^2(c+V)} + \frac{g}{V(c+V)} \right] \frac{I}{(\lambda_1 \phi)} = \frac{C_5 g}{Vc} \quad (31)$$

Hence

$$\frac{d\phi}{ds} + \phi \left[\frac{g}{Vc} \frac{dy}{ds} + \frac{g}{V(c+V)} \frac{dy}{ds} + \frac{C_5 g}{c} \frac{dt}{ds} \right]_I = 0$$

or, after integration

$$\log\phi \Big|_I + \int_I \frac{g(2c+V)}{Vc(c+V)} dy + \left[\frac{C_5 g t}{c} \right]_I^2 = 0 \quad (32)$$

This holds provided that, from Eqs. (30) and (31)

$$D' \frac{V}{c} \exp\left(\frac{V}{c} - \frac{y}{H}\right) = \phi \left[\frac{g}{V(c+V)} \sin\gamma + \frac{C_5 g}{Vc} \right] \quad (33)$$

The similarity with Tsien and Evans' case for the vertical, $\sin\gamma = 1$ and $C_5 = 0$ can be seen immediately. The drag-to-mass variation is given by

$$D' V^2 \exp\left(-\frac{y}{H}\right) = Mg \left[\frac{c}{(c+V)} \sin\gamma + C_5 \right] \quad (34)$$

Also, from Eqs. (31) and (27)

$$\begin{aligned} \frac{g}{V(c+V)} \left[\frac{2c}{V} C_2 + I \right] &= C_5 \frac{g}{Vc} (\lambda_1 \phi) \\ &= C_5 \frac{g}{Vc} \left(\frac{Vc}{Vc - gH} \right) [C_3 + C_4 \tan\gamma] \end{aligned}$$

Hence

$$C_3 + C_4 \tan\gamma = \frac{(Vc - gH)}{V(c+V)} \frac{I}{C_5} \left[\frac{V + 2cC_2}{V} \right] \quad (35)$$

The term in gH/c is negligibly small, being only of the order of 28 m/s relative to velocities of hundreds or even thousands of m/s. Assuming that, in Eq. (35), $2C_2 = 1$, the terms in $(c+V)$ disappear. This assumption can only affect the angle turned through by the flight path, which can be freely chosen by choosing correctly the initial flight path angle. Thus, depending on the sign of C_3 the equations become

$$\begin{aligned} C_3 + C_4 \tan\gamma &= I/C_5 \cdot c/V \\ \tan\gamma &= (a + bc/V) \end{aligned} \quad (36)$$

Equation (36) shows that the solution of the optimal equations has the correct form for simple integration as shown by Eqs. (15) and (16). The fuel consumed follows from Eq. (32) and the drag/mass ratio from Eq. (34).

Equation (34) gives the value of C_5 , the constant in the time-of-flight equation.

$$C_5 = \frac{D' V_I^2}{M_0 g} \exp\left(\frac{V_I}{c}\right) - \frac{c}{(c+V_I)} \sin(\gamma_I) \quad (37)$$

Thus C_5 can be positive, zero, or negative depending on the magnitude of the right-hand side of Eq. (37).

Conclusion

A simple and satisfactory method for finding the optimal climb path of a ballistic rocket within the atmosphere has been derived. The resulting equations are solvable by simple quadrature. The optimal solution requires an impulsive boost to start the trajectory and variable thrust to complete it, otherwise no optimization can be carried out.

References

- ¹Tsien, H.S. and Evans, R.C., "Optimum Thrust Programming for a Sounding Rocket," *Journal of the American Rocket Society*, Vol. 21, Sept. 1951, pp. 99-107.
- ²Leitman, G., (ed.), *Optimization Techniques - With Application to Aerospace Systems*, Academic Press, New York, 1962.
- ³Large, E., "Optimal Flight Paths for a Winged, Supersonic Rocket Vehicle," *Journal of the Royal Aeronautical Society*, Dec. 1978.

Computational Scheme for Calculating the Plume Backflow Region

Basil P. Cooper Jr.*

McDonnell Douglas Astronautics Company,
Huntington Beach, Calif.

Introduction

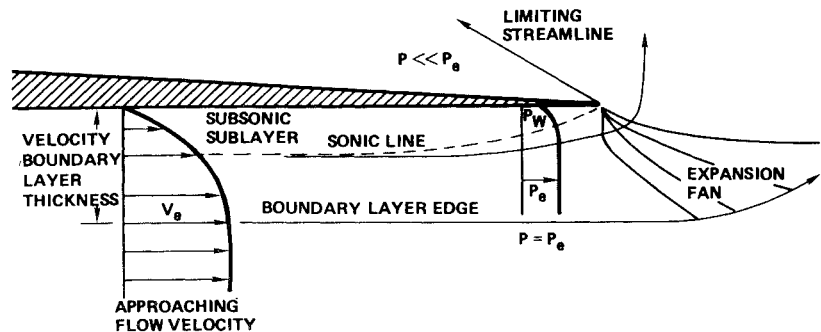
SEVERAL computer programs and approximate methods exist for the calculation of rocket engine exhaust plume flowfields. The majority of these computational schemes neglect the effects of the nozzle wall boundary layer on the plume flowfield and, therefore, are useful mainly for calculating the core flowfield of the plume. This restriction is usually unimportant since most of the mass contained within

Presented as Paper 78-1631 at the AIAA/IES/ASTM 10th Space Simulation Conference, Bethesda, Md., Oct. 16-18, 1978; submitted Jan. 10, 1979; revision received April 20, 1979. Copyright © American Institute of Aeronautics and Astronautics, Inc., 1979. All rights reserved.

Index categories: Computational Methods; Supersonic and Hypersonic Flow.

*Senior Engineer/Scientist. Member AIAA.

Fig. 1 Boundary-layer flow near the nozzle lip.



the plume is in this core region. However, this limitation is unacceptable for applications where a surface which can be adversely affected by plume impingement forces, heating, or contamination is located behind the nozzle exit plane in what is called the "plume backflow region." The flow in this region originates in, and is highly affected by, the nozzle wall boundary layer in the calculations. This paper presents the results of modifications of a method-of-characteristics computer program to include the effects of the nozzle wall boundary layer on the plume flowfield.

Program Modification and Use

The computer program chosen for modification was the Variable Oxidizer to Fuel (O/F) Ratio Method of Characteristics (VOFMOC) program.¹ The VOFMOC computer program uses a method-of-characteristics computational scheme to calculate the plume flowfield. It is capable of including real gas effects in its computations, as well as the effects of a simplified nozzle wall boundary layer. The program does not, however, include the effects of the thermal boundary layer, which is associated with a cooled nozzle wall, and it neglects the effects of the subsonic portion of the boundary layer. VOFMOC was modified to permit the input of separate velocity and thermal boundary-layer profiles at the nozzle exit plane, and a treatment of the subsonic portion of the boundary layer was added.

In the modified program, the subsonic portion of the boundary layer is treated in a manner similar to that used for supersonic and hypersonic flow approaching a sharp corner where a large pressure gradient exists.^{2,3} The assumption is made that the ambient pressure external to the nozzle is very much lower than the pressure at the edge of the nozzle boundary layer at the exit plane, P_0 . When this assumption is valid, it has been shown, both experimentally⁴ and analytically,^{5,6} that the effect of the very-high-pressure gradient at the nozzle lip is to accelerate the subsonic portion of the boundary layer so that the sonic line intersects the nozzle lip, as shown in Fig. 1. Under these circumstances, the no-slip assumption, which is usually made in boundary-layer analysis, is not valid at the nozzle lip. In addition, the viscous effects become important only in a negligibly thin sublayer of the boundary layer; therefore, inviscid flow equations may be employed in the flow expansion around the corner. At the exit plane of the nozzle, therefore, the boundary-layer flow can be represented as a completely supersonic flow with the flow Mach number equal to 1.0 at the nozzle wall. Also at the nozzle wall, the flow stagnation temperature and stagnation

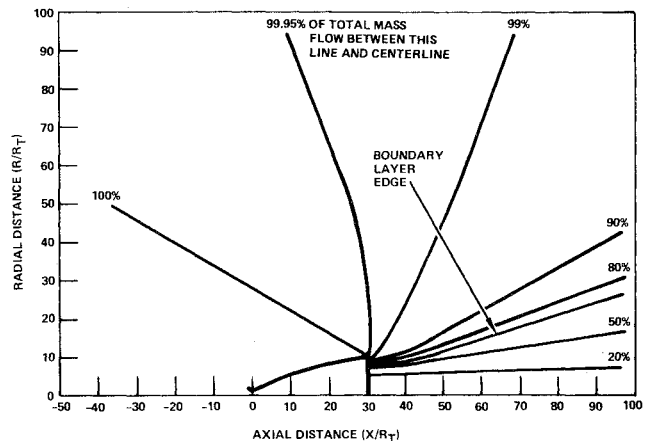


Fig. 2 Calculated plume streamlines for 22.24 N bipropellant engine.

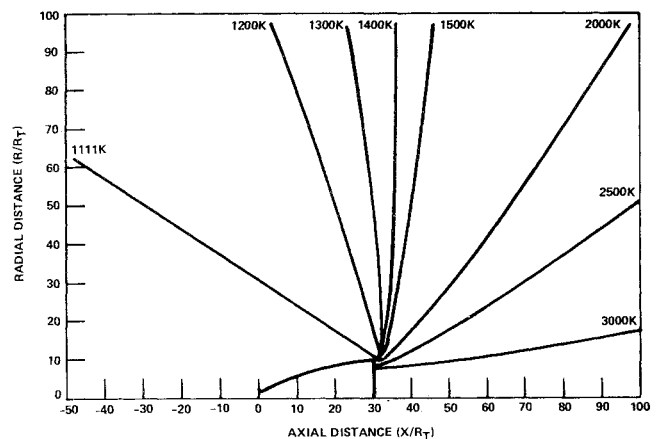


Fig. 3 Stagnation temperature contours for a 22.24 N bipropellant engine.

pressure are equal to the nozzle wall temperature and the boundary-layer edge pressure, T_w and P_0 , respectively, since this flow on the wall was stagnated a few boundary-layer thicknesses upstream of the lip where the no-slip assumption is still valid.

The modified program has been named VISMOC in order to distinguish it from VOFMOC. To use VISMOC, a user inputs the velocity and stagnation enthalpy profiles, the velocity and thermal boundary-layer thicknesses, and a set of thermodynamic properties which covers the range of stagnation conditions encountered in the boundary layer. These inputs may be obtained from standard boundary-layer and thermochemistry computer programs. The program uses these inputs to calculate the flow properties for a method-of-characteristics start-line at the nozzle exit and the remaining calculations are made as if the flow were inviscid.

Table 1 Baseline operating conditions

Parameter	Value
Oxidizer/fuel ratio	1.6
Combustion chamber pressure	6.80 atm (100 psi)
Nozzle area ratio	100
Throat radius R_T	0.218 cm (0.086 in.)

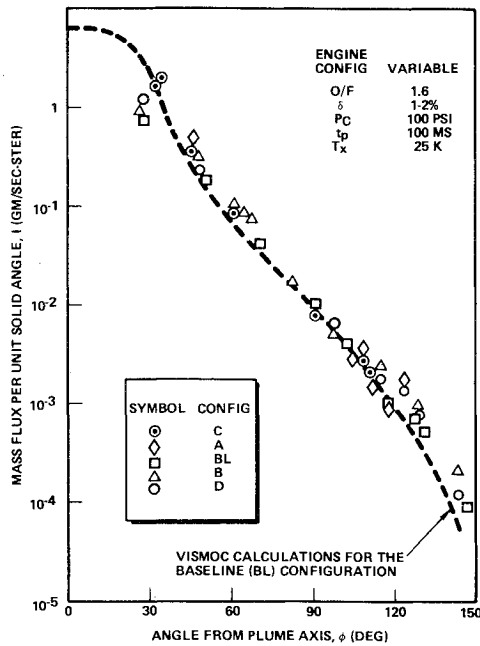


Fig. 4 VISMOC calculations compared to mass flux test data from 22.24 N bipropellant engine.

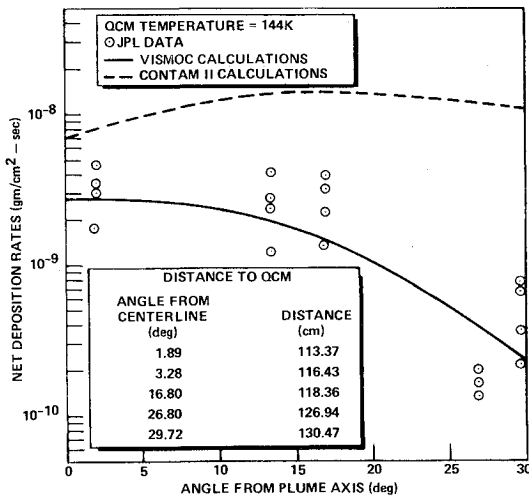


Fig. 5 Mass deposition rates from a 0.89 monopropellant engine for a QCM temperature of 144 K.

Comparison with Experimental Results

The VISMOC program was used to calculate the flowfield from a 22.24 N (5 lb_f) bipropellant thruster recently tested by Scott, et al.⁷; the results of these calculations were compared with the experimental data. The thruster was operated under a variety of conditions and at two nozzle area ratios.⁷ The calculations were made for the baseline conditions which are shown in Table 1. In the calculations, the nozzle wall temperature was assumed to be 1111 K (2000°R), the nozzle boundary layer was assumed to have a laminar profile, and the thickness used was that given in Ref. 7 as 18.8% of the nozzle exit radius.

The results of the VISMOC calculations for the plume streamlines are shown in Fig. 2. The figure depicts the percentages of the total plume mass flux contained between the plume centerline and the various streamlines. It is readily apparent that only a small portion of the nozzle exhaust enters the plume backflow region. The reduction in the flow stagnation temperature, due to the heat transfer through the

boundary layer to the nozzle wall, is shown in Fig. 3. In Fig. 4, the calculated mass flux as a function of angle from the plume axis is compared with the values measured.⁷ The agreement with the data is seen to be very good. The VISMOC program was also used to calculate the plume flowfield for a 0.89 N (0.2 lb_f) monopropellant thruster.⁸ The calculated mass fluxes were used to determine the mass deposition rates which could be expected on quartz crystal microbalances (QCM's) kept at constant temperatures of 172 K and 144 K. The deposition rates were calculated in a manner similar to that used by Davis and Wax⁹ when they compared the predictions of the CONTAM II computer program with the data reported in Ref. 8. Figure 5 shows the comparison of the VISMOC calculations with the data of Ref. 8 and the CONTAM II calculations of Davis and Wax for the QCM temperature of 144 K. Although there is considerable scatter in the data, the agreement of the VISMOC calculations with the data is still quite good. The comparison of the VISMOC calculations to the data for the QCM temperature of 172 K was equally good.

Conclusions

The VOFMOC computer program has been modified to predict the effects of the nozzle boundary layer on the plume backflow region and limited comparisons of calculated results and experimental data have been made. The comparisons of the VISMOC calculations with the experimental data indicate that the VISMOC computer program may be a useful tool for calculating the entire plume flowfield for liquid propellant rocket engines.

Acknowledgments

Much of the work in modifying the VOFMOC computer program was performed with the technical cognizance of T.F. Greenwood and D.C. Seymour under NASA Contracts NAS8-21810 and NAS8-31644 to Northrop Services, Inc., Huntsville, Ala. The remainder of the work reported in this paper was performed under MDAC independent research and development funding.

References

- Smith, S.D. and Ratliff, A.W., "Variable O/F Ratio Method of Characteristics Program for Nozzle and Plume Analysis," *Rocket Exhaust Plume Computer Program Improvement*, Vol. 1, Final Rept., LMSC/HREC D162220-I, HREC-7761-1, Lockheed Missiles and Space Co., June 1971.
- Fishburn, D.B. and Adamson, T.C., Jr., "Transonic Region of a Supersonic Boundary Layer Turning a Sharp Corner," *AIAA Journal*, Vol. 10, Feb. 1972, pp. 123-124.
- Olsson, G.R. and Messiter, A.F., "Hypersonic Laminar Boundary Layer Approaching the Base of a Slender Body," *AIAA Journal*, Vol. 7, July 1969, pp. 1261-1267.
- Hama, F.R., "Experimental Investigations of Wedge Base Pressure and Lip Shock," Jet Propulsion Laboratory, California Institute of Technology, TN-32-1033, 1966.
- Matveeva, N.S. and Neiland, V.I., "Laminar Boundary Layer Near a Corner Point of a Body," *Akademiia Nauk SSSR, Izvestiia, Mekhanka Zhidkosti i Gaza*, Vol. 4, 1967, pp. 64-70.
- Olsson, G.R. and Messiter, A.F., "Acceleration of a Hypersonic Boundary Layer Approaching a Corner," University of Michigan, Willow Run Laboratories of the Institute of Science and Technology, Rept. 8416-13-T, May 1968.
- Scott, H.E., Frazine, D.F., and Lund, E.G., "Bipropellant Engine Plume Study," USAF/NASA International Spacecraft Contamination Conference, U.S. Air Force Academy, Colo., March 1978.
- Baerwald, R.K. and Passamaneck, R.S., "Monopropellant Thruster Exhaust Plume Contamination Measurements," Air Force Rocket Propulsion Laboratory, AFRPL-TR-77-44, Sept. 1977.
- Davis, L.P. and Wax, S.G., "Verification of Contamination Predictions for Monopropellant Thrusters," Air Force Rocket Propulsion Laboratory, AFRPL-TR-77-56, Oct. 1977.